P1.40   ARCTIC SEA ICE CHANGES AND FUTURE ACCESS FOR MARINE NAVIGATION

Lawson W. Brigham
U. S. Arctic Research Commission, Arlington, VA

Michael S. Timlin* and John E. Walsh
Department of Atmospheric Sciences, University of Illinois, Urbana, IL

1. INTRODUCTION

In assessments of ongoing and projected climate change, sea ice is a critical element. Not only is sea ice an indicator of climate change through its integration of thermodynamic and dynamic forcing of the high-latitude surface, but it is also an agent of climate change through feedbacks involving the coupled atmosphere-ocean-ice system. Global climate models simulate the coupling and, in principle, the feedbacks involving sea ice. Unfortunately, the coarse resolution and simplified parameterizations in these models introduce systematic errors into the simulations of the atmosphere, the ocean and sea ice. These errors can be evaluated in simulations of the present climate by comparing the simulations with observational data. However, such errors present significant challenges in the use of these models to simulate climate change, since the models are essentially being asked to capture changes from flawed initial states. The IPCC (2001) and other assessments of future climate change have devoted considerable attention to the uses of these models for projections of climate change over the next several decades to a century. Effective uses of model projections are especially important in such efforts because models are the most powerful tools available for projecting climate changes. Alternative statistical approaches and analogs to past climate change are highly questionable in the present situation, when anthropogenically-driven changes in greenhouse concentrations are occurring at unprecedented rates.

The Arctic Climate Impact Assessment (ACIA, http://www.acia.uaf.edu/) is an international effort, coordinated by the International Arctic Science Council, to evaluate ongoing and projected changes in the Arctic climate system. Changes in sea ice are of major importance in ACIA, not only because of the roles of sea ice in the climate system, but also because of potentially important impacts of future changes of sea ice: new opportunities for navigation and offshore industry, changes in marine ecosystems, and changes in coastal erosion and perhaps Arctic storminess. A scenario working group appointed by ACIA identified five global climate models as sources of information on projected changes in the Arctic climate system. These models, selected on the basis of documentation in the refereed literature and on the basis of the availability of archived output, are listed below, together with references providing information on the models:

• Canadian Climate Centre for modeling and analysis, CCCma (Flato et al. 2000)

• Geophysical Fluid Dynamics Laboratory, GFDL (Knutson et al. 1999)

• European Centre/Hamburg Max-Planck-Institute, ECHAM (Roeckner et al. 1999)

• Hadley Centre for Climate Prediction and Research, Climate Model version 3, HadCM3 (Gordon et al. 2000)

• National Center for Atmospheric Research, Climate System Model, NCAR (Boville et al. 2001)

All five models have been used in greenhouse simulations employing the IPCC's B2 forcing scenario, which represents a more modest rate of increase of greenhouse gas concentrations than does its counterpart, the A2 scenario (IPCC 2000). The B2 scenario simulations generally begin in the mid-to-late 20th century with historical forcing, and then continue through 2100 with the B2 forcing. The CCCma model was used for three different simulations of the 1975-2100 period; the three ensemble members differ as a result of perturbations of the initial conditions. The archives of all the model simulations include monthly grids of sea ice coverage, in addition to monthly (and sometimes daily) grids of many other variables, including surface air temperature. The monthly output was used in the present evaluation.

2. RESULTS

All five models project increases in Arctic surface air temperature and decreases of Arctic sea ice coverage. Figure 1 shows the 21st-century time series from the various models, all in the form of 11-year running means of the surface air temperature averaged over 60-90°N. The warming by the end of the century ranges from approximately 3.5°C in the NCAR model to approximately 5.5°C in the ECHAM model. For comparison, the projected increases of global mean temperature range from about 1.2°C in the NCAR model to about 2.5°C in

* Corresponding author address: Michael S. Timlin, Department of Atmospheric Sciences, University of Illinois, 105 S. Gregory St., Urbana, Illinois 61801; e-mail: timlin@atmos.uiuc.edu
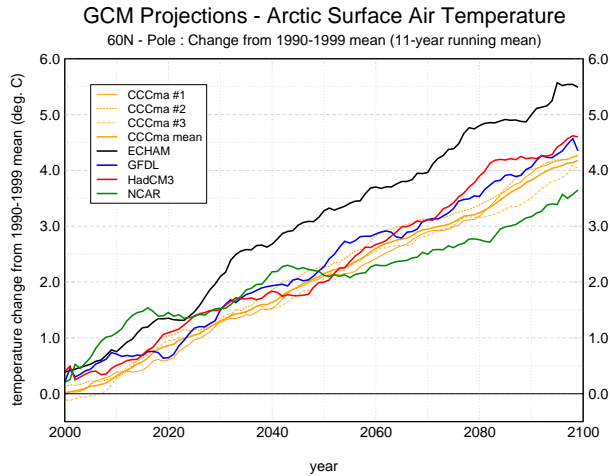
GCM Projections - Arctic Surface Air Temperature
60N - Pole : Change from 1990-1999 mean (11-year running mean)

Figure 1. Projected changes of Arctic surface air temperature (°C), averaged over 60-90°N, from five global climate models identified in legend. Changes are relative to each model's mean value for 1990-1999 and are plotted as 11-year running means centered on indicated year. Results from CCCma model are shown for three individual ensemble members (broken orange lines) and for the three-member ensemble mean (solid orange line).

the projections of sea ice cover throughout the 21st century. In some cases, the biases of the present-day extent are actually larger than the changes projected by the same models over the 2000-2100 period.

Because the present-day biases are large, they can dominate estimates of ice extent based on the raw output of a particular model. If one is willing to assume that there is some useful information in the rates of change of the ice coverage in the model simulations – an assumption that is clearly open to question – then the model-derived estimates of future ice cover can be enhanced by adjustments for the biases in the initial (circa 2000) simulated extents. In effect, this strategy superimposes the simulated variations and trends onto the "correct" initial sea ice state of each simulation of the 21st century. The implementation of this strategy is complicated somewhat by the fact that the models' systematic errors are larger in some regions than in others. Accordingly, the procedure followed here is an adjustment of each model's simulated ice extent on the basis of that model's bias of present-day (1980-1999) extent, relative to the corresponding observed extent, in each calendar month and at each longitude (in 1° increments). The source of the observational data was the Hadley Centre's Had-ISST dataset, version 1.1 (Rayner et al. 1999). The sea

the ECHAM, HadCM3 and CCCma models. These global warmings are in the lower portion of the 1.5°-4.5°C range in the IPCC's (2001) recent assessment, confirming that the B2 scenario of forcing is less extreme than the "business-as-usual" scenarios such as A2.

Figure 1 also shows that the three members of the CCCma ensemble produced similar changes of Arctic temperature. In fact, the three CCCma time series are more similar to each other than to any of the other models' time series. This similarity of the three ensemble members was found in the simulations of other variables, including sea ice. Hence we present the CCCma sea ice results in the form of averages of the output from the three ensemble members, thereby homogenizing the display of the results.

Figure 2 shows the time series of the simulated ice extent from each model for March and September, the calendar months of maximum and minimum sea ice extent in the Arctic. The general decrease of sea ice in the 21st century is common to the models, although interannual to decadal variations are superimposed on the decreases. However, an outstanding feature of Figure 2 is the spread of the present-day simulations. Figure 2a shows that the simulated ice extent varies from 14 to 20 million km^2 in March, and from 2 to nearly 12 million km^2 in September. The corresponding observed ice extents, based on satellite passive microwave measurements, are approximately 16 and 8 million km^2, respectively. The biases of the individual models are sufficiently large that they represent significant contaminations of
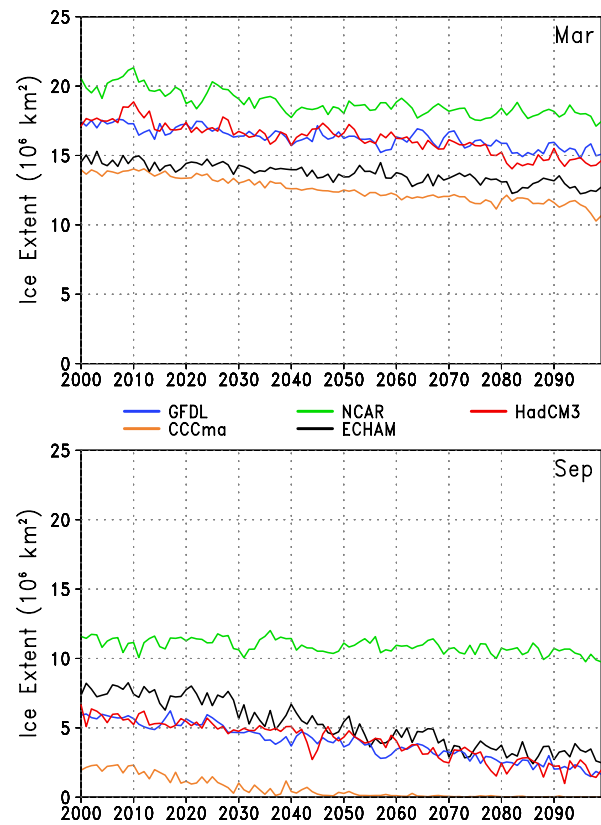

Figure 2. Time series of March (upper) and September (lower) ice extents simulated by the five global climate models (see legend between panels). The ice extents are unadjusted.
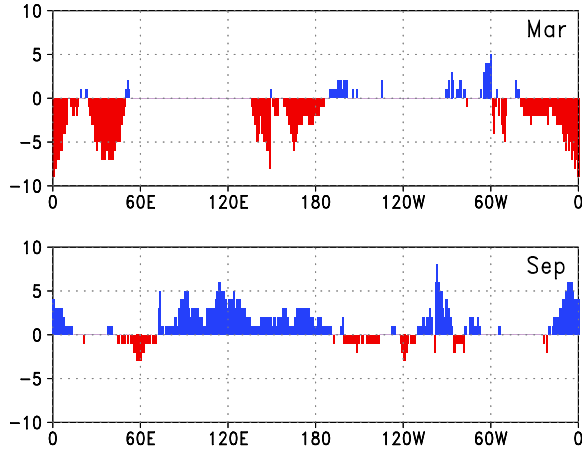
Figure 3. Longitudinal distributions of the adjustments applied to ice extent simulated by the HadCM3 model in March (upper panel) and September (lower panel). Negative (red) values denote removal of oversimulated ice, positive (blue) values denote addition of undersimulated ice.

ice information in HadISST for the 1980-1999 period is based largely on satellite passive microwave measurements (Cavalieri et al. 1997). The adjustment procedure is essentially an addition or removal of sea ice at each longitude by an amount equivalent to the negative of the bias at the particular longitude and calendar month. This procedure is different from the so-called "flux adjustment" often employed in coupled global model simulations, since the procedure used here simply imposes *a posteriori* or *ad hoc* modifications of the model output; the model simulations are unaffected by the adjustments. As with flux adjustments, however, our procedure implicitly assumes that the optimal adjustments do not change with time – an assumption that is almost certainly subject to some error.

As an example of the adjustment of ice extent, Figure 3 shows the longitudinal dependence of the adjustment (in ° latitude) to HadCM3's sea ice in March and September. Where the model over-simulates sea ice, the adjustment is negative (red). Where the model under-simulates ice, the adjustment is positive (blue). It is apparent that HadCM3's bias is strongly dependent on longitude and season, although the bias is generally positive in March and negative in September. The adjustments at some longitudes exceed five degrees of latitude, as in the downward adjustment of the model's March ice extent in the eastern North Atlantic subpolar seas (20°W-50°E).

Figure 4 shows the 21st-century time series of each model's adjusted ice extent for March and September. The adjusted time series show much less spread among themselves than do the unadjusted time series in Figure 2, since the models now have a common "starting point". (Figure 4's extents in the year 2000 differ slightly
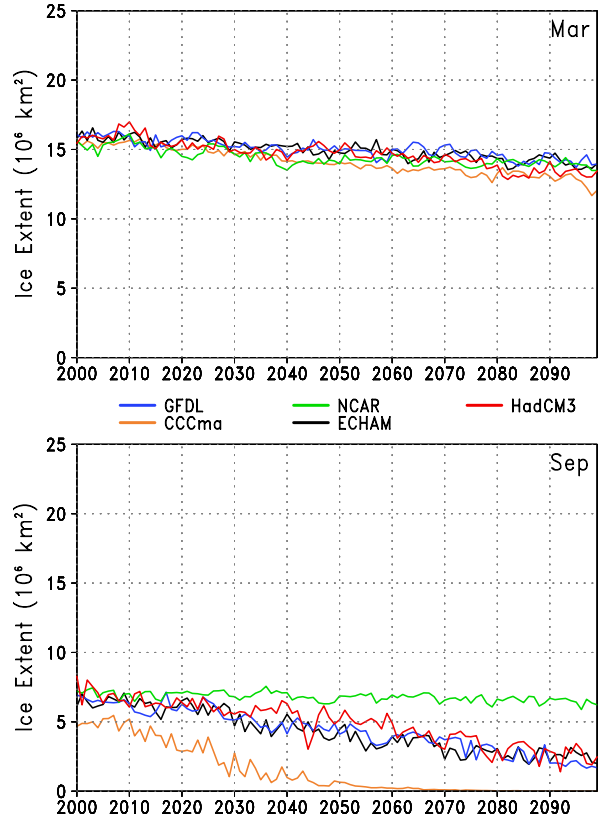

Figure 4. As in Figure 2, but for the ice extents after adjustments for the present-day biases.

because the adjustments are based on the means over 1980-1999, which are not exactly the same as the year-2000 values).

While the March extents vary little among the models in the adjusted time series (Figure 4a), the September extents (Figure 4b) develop somewhat more spread by 2100. The most ice is projected by the NCAR model, in which the present-day Arctic is coldest. The least ice in September is projected by the CCCma model, which simulates the warmest present-day climate of the Arctic. The CCCma model deserves special mention because its simulation became ice-free in September by approximately 2060 (Figure 2b). This model's present-day bias was quite negative in September, so the positive adjustment effectively led to a constant (nonzero) ice cover beyond 2060. Our adjusted time series in Figure 4b is based on a continuation of the pre-2050 rate of decrease into the period beyond 2050, so the adjusted values erode at the same rate as the unadjusted ice – leading to ice-free Septembers in CCCma by the 2070s.

The net changes of annual mean Northern Hemisphere sea ice are summarized in Table 1. The changes are presented as actual areal changes (10^6 km^2) and as percentage changes from the initial values of both the adjusted and unadjusted time series. The percentage changes vary from about 14% to 42% in the unadjusted

Table 1. Changes of annual mean Northern Hemisphere ice extent, 1980-99 to 2080-99.

model	change, 10^6 km^2 (unadjusted)	% change (unadjusted)	change, 10^6 km^2 (adjusted)	% change (adjusted)
CCCma	from 9.7 to 5.6	-42%	from 12.3 to 6.6	-46%
ECHAM	from 11.9 to 8.9	-25%	from 12.3 to 9.3	-24%
GFDL	from 11.9 to 8.5	-29%	from 12.3 to 8.6	-30%
HadCM3	from 12.8 to 9.4	-27%	from 12.3 to 9.1	-26%
NCAR	from 16.5 to 14.2	-14%	from 12.3 to 10.8	-12%

time series, and from about 12% to 46% in the adjusted time series. These percentages would be smaller if they were based solely on the winter time series, and larger if based solely on summer values, as one may infer from Figure 4.

Finally, Figure 5 provides spatial distributions of the simulated sea ice by showing the number of models in which sea ice is present during 2070-2090 at each location in March and September, in both the adjusted and unadjusted results. Figures 5c and 5d both show the narrowing of the spread achieved by the adjustment. Figure 5c, in particular, shows that wintertime sea ice over the Arctic Ocean and various peripheral seas persists through the late 21st century in all models, at least according to the adjusted output of the B2 simulations. While these distributions say nothing about the ice thickness, they do indicate that the reductions of winter ice extent are quite modest in the B2 scenarios. The summer extents show greater inter-model variations and more substantial reductions (Figures 5b, 5d). One implication of Figure 5d is that navigational opportunities will be greatly increased in the Arctic Ocean during summer, since large areas of the Arctic Ocean are ice-free for at least part of the summer in most of the models.
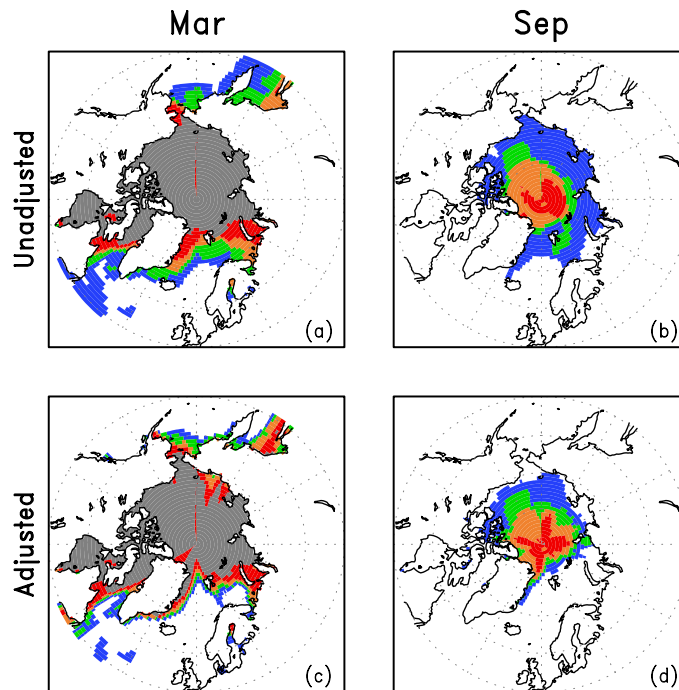

Figure 5. Geographical distribution of the coverage of sea ice during March (left panels) and September (right panels) in the 2070-2090 time slice. Colors denote numbers (out of 5) of the models in which sea ice was present: blue = 1, green = 2, orange = 3, red = 4 and gray = 5. Upper panels are for unadjusted extents and lower panels are for adjusted extents.

3. APPLICATION TO THE NORTHERN SEA ROUTE

The large areas of open water indicated in Figure 5 suggest that the Arctic Ocean will become considerably more accessible to marine operations by the end of the 21st century. As a first attempt toward quantifying this increase of navigability, we focus on the Northern Sea Route, consisting of the seas offshore of northern Russia. This route offers the advantage of a much shorter distance (and transit time) between the North Pacific and Europe than alternative routes through the Panama Canal and the North Atlantic, or across the Indian Ocean south of the Asian landmass. We chose to focus on the Northern Sea Route because it is more easily resolvable by global climate models than is the "Northwest Passage" through the Canadian Archipelago, where the complex juxtaposition of narrow straits and islands requires resolution much finer than the 200-300 km typical of the model simulations employed here.

Changes in the length of the Northern Sea Route's navigation season were evaluated from the model output in two ways. First, we calculated for each year the number of consecutive days in which there was at least one open-water grid cell north of all points between the Bering Strait and Novaya Zemlya. (An open-water grid cell was defined here as one in which the ice concentration was 50% or less). Second, we repeated the calculation

Northern Sea Route:
Navigability projected for 2000-2100

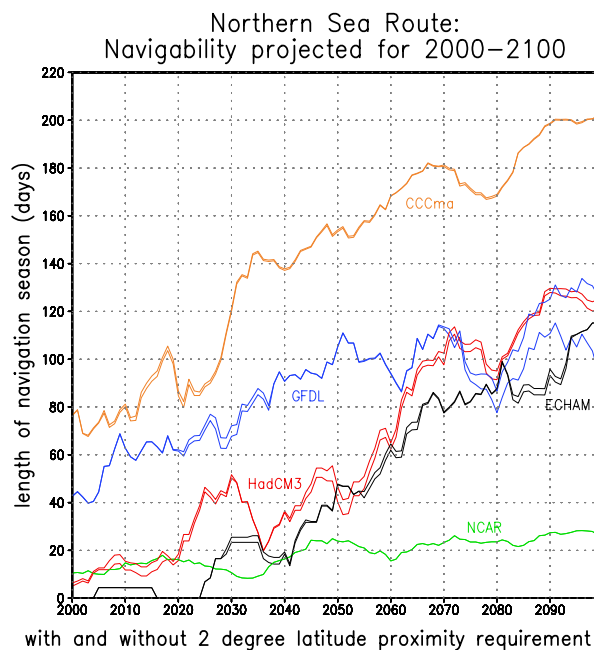with and without 2 degree latitude proximity requirement

Figure 6. Lengths (days) of navigation seasons projected for the Northern Sea Route. Values are shown as 10-year running means for the 21st century. Two curves for each model represent the season lengths with (upper curve) and without (lower curve) the requirement that open water at adjacent longitudes be within 2° latitude (see text).

with the additional requirement that the open-water grid cells north of adjacent coastal points must be within 2° latitude, thereby imposing in a simplistic way the requirement that the open-water grid-cells comprise a more-or-less continuous route.

Figure 6 shows the time series of the duration of the navigation season derived from the adjusted sea ice output from each global climate model. (For each model, the lower curve in Figure 6 was obtained by the method in which the 2°-latitude proximity requirement was imposed for adjacent open-water cells). It is apparent that, by the late 21st century, the navigation season is projected to lengthen by an average (over the five models) of 60-90 days. However, the lengthening ranges from only about 10 days in the model (CSM) with the smallest ice retreat to as much as 120 days in the model (CCC) with the greatest ice retreat. In most of the model simulations, the retreating ice continues to interact with the northern tip of Severnaya Zemlya, implying a reliance on a transit route through Vilkitski Strait between the Kara and Laptev Seas. These mean values do not convey information about interannual or decadal variations, which can be substantial. Foe example, Figure 6 shows that the length of navigation season can actually decrease for decadal-scale periods (e.g., the 2070s in the HAD, CCC and GFD models), presumably because of the inherent natural variability of the climate simulated by the models.

The results in Figure 6 are preliminary in the sense that their sensitivities to the computational algorithm and to various parameters have not been explored. For example, it may be possible for ships to navigate effectively through ice concentrations of 75% or greater. The use of a 75% threshold, rather than the 50% used here, will likely impact the numerical values of the navigation season length. Future analyses will be sure to determine the influence of ice concentration threshold on the resulting ice navigation season.

4. CONCLUSION

The following are the highlights of the results presented here:

• Projections of 21st-century ice extent by coupled global models are strongly dependent on, if not dominated by, the models' simulations of present-day ice extent.

• Adjustments based on biases of the simulated present-day ice extent narrow the spread among the model projections, subject to the caveat that adjustments are strictly *ad hoc*, non-physical and open to question concerning the validity of the assumption of temporal invariance over the 100-year timeframe.

• The model with the most ice in its control climate has the smallest percentage loss (as well as the smallest absolute loss) of ice over the 21st century; the model with the least ice in its control climate has the largest loss of ice by 2100. However, this finding does not rep-

resent a universal rule; for example, it is not valid if one compares the HadCM3 and ECHAM models (Table 1).

• The models with the warmest (coldest) present-day Arctic climate show the largest (smallest) reductions of ice extent, even after the adjustments are imposed.

• The navigation season of the Northern Sea Route is projected to lengthen by an average (across the models) of 60-90 days by the end of the 21st century. However, the estimates of the lengthening vary widely among the models, from as little as about 10 days to as much as about 120 days and the results are dependant on various parameters used to calculate the navigation season length.

Despite the *ad hoc* nature of the adjustments applied here, the adjusted sea ice distributions should be more useful for applications such as the Arctic Climate Impact Assessment, which requires "best estimates" of the future distribution of sea ice. We believe that the adjusted ice extents, while still flawed, are more credible than the unadjusted estimates because one obvious source of error (biases in the initial state) have been addressed, albeit in a non-physical way. It should be noted that the procedure used here is not the only possible method for adjusting the simulated ice coverage; for example, one could perform sea ice simulations "off-line" using observed initial conditions for sea ice (e.g., the year-2000 distribution) and forcing from the atmospheric component of a climate model's simulation of the 21st century.

As coupled climate models become more realistic, the magnitude of the required adjustments will almost certainly decrease. The adjustments are already relatively small in some of the models used here. However, biases and the potential for enhancement by adjustment are likely to persist on the regional scale for the foreseeable future.

REFERENCES

Boville, B. A., Kiehl, J. T., Rasch, P. J. and Bryan, F. O., 2001: Improvements to the NCAR CSM-1 for transient climate simulations. *J. Climate*, **14**, 164-179.

Cavalieri, D. J., Gloersen, P., Parkinson, C. L., Comiso, J. C. and Zwally, H. J., 1997: Observed hemispheric asymmetry in global sea ice changes. *Science*, **278**, 1104-1106.

Flato, G., Boer, G. J., Lee, W. G., McFarlane, N. A., Ramsden, D., Reader, M. C. and Weaver, A. J., 2000: The Canadian Centre for Climate Modelling and Analysis global coupled model and its climate. *Clim. Dyn.*, **16**, 451-468.

Gordon, C., Cooper, C., Senior, C. A., Banks, H. T., Gregory, J. M., Johns, T. C., Mitchell, J. F. B. and Wood, R. A., 2000: The simulation of SST, sea ice extents and ocean heat transports in a variation of the Hadley Centre coupled model without flux adjustments. *Clim. Dyn.*, **16**, 147-168.

IPCC, 2001: *Climate Change 2001: The Scientific Basis* (Houghton, J. T., Ding, Y., Griggs, D. J., Noguer, M., van der Linden, P. J., Dai, X., Maskell, K. and Johnson, C. C., Eds.), Contribution of Working Group I to the Third Assessment Report of the Intergovernmental Panel on Climate Change, Cambridge University Press, Cambridge, UK.

IPCC, 2000: *Special Report on Emission Scenarios: A Special Report of Working Group III of the Intergovernmental Panel on Climate Change* (Nakicenovic, N. J., Alcamo, J., Davis, G. and 25 others, Eds.), Cambridge University Press, Cambridge, UK.

Knutson, T. R., Delworth, T. L., Dixon, K. W. and Stouffer, R. J., 1999: Model assessment of regional surface temperature trends (1949-1997). *J. Geophys. Res.*, **104**, 30981-30996.

Rayner, N.A., Parker, D.E., Frich, P., Horton, E.B., Folland, C.K. and Alexander, L.V., 2000: SST and sea-ice fields for ERA40 In: Proceedings of the Second WCRP International Conference on Reanalyses (Wokefield Park, Reading UK August 1999), WCRP-109, WMO/TD-No 985.

Roeckner, E., Bengtsson, L., Feichter, J., Lebeveld, J. and Rodhe, H., 1999: Transient climate change simulations with a coupled atmosphere-ocean GCM including the tropospheric sulfur cycle. *J. Climate*, **12**, 3004-3012.